Optical rotation in thin chiral/twisted materials and the gyrotropic magnetic effect

Yan-Qi Wang [1,2] Takahiro Morimoto,[3,4] and Joel E. Moore[1,2]

[1]*Department of Physics, University of California, Berkeley, California 94720, USA*
[2]*Materials Sciences Division, Lawrence Berkeley National Laboratory, Berkeley California 94720, USA*
[3]*Department of Applied Physics, The University of Tokyo, Hongo, Tokyo, 113-8656, Japan*
[4]*JST, PRESTO, Kawaguchi, Saitama, 332-0012, Japan*

The rotation of the plane of polarization of light passing through a nonmagnetic material is known as natural optical activity or optical gyrotropy. The behavior of this effect in thin chiral conductors is of current interest. For example, the low-frequency limit of gyrotropy in chiral three-dimensional (3D) crystals, known as the gyrotropic magnetic effect (GME), is controlled by the orbital magnetic moment of electrons, which has been proposed to be relevant to current-induced switching in twisted bilayer graphene. We show that the GME is not limited to bulk materials but also appears for quasi-2D systems with minimal structure incorporated in the third direction. Starting from multiband Kubo formula, we derive a generic expression for GME current in quasi-2D materials induced by low-frequency light, and provide a Feynman-diagrammatic interpretation. The relations between the 2D finite layered formula and 3D bulk formula are also discussed.

I. INTRODUCTION

The breaking of symmetry in a medium between polarized light with different chiralities is called optical gyrotropy, leading to the rotation of the polarization plane in propagation [1]. Faraday rotation and magnetic circular dichroism, for instance, are time-reversal-odd gyrotropic effects and appear at zeroth order in the wave vector of light. At linear order in wave vector, the time-reversal-even part of the optical response is called natural gyrotropy, whose dissipative part leads to natural circular dichroism, while the reactive part gives the optical rotation known as natural optical activity [1–4].

Recently the mechanism of these effects at low frequencies has been of considerable interest. Beyond merely probing a material's symmetry, the low-frequency limit of natural gyrotropy in chiral three-dimensional (3D) metals turns out to probe a very basic property of Bloch electrons, in a loosely similar way to electric polarization and other Berry-phase phenomena. This limit was named the gyrotropic magnetic effect (GME) [3], as it includes as a special case one version of the previously discussed chiral magnetic effect in Weyl semimetals [5–8]. It is controlled by the intrinsic orbital magnetic moment of the electrons on the Fermi surface [3,8,9], which is determined by the Bloch states and is related to but distinct from the more familiar Berry curvature. The GME has recently been studied in Weyl semimetals by first-principles calculations [10,11]. While there are clearly a variety of nonlinear effects in Weyl semimetals known to be interesting and even approximately quantized [5–7,12–18], the GME remains a relatively straightforward probe of chirality as it is a linear response.

The motivation for this paper is to understand how the simplest electromagnetic response to chirality in a time-reversal-invariant system, the GME, is modified in a minimal chiral structure, such as a stack of a few rotated layers, rather than a bulk crystal. The optical phenomena in thin conductors, with minimal structure incorporated in the third direction, is of great current interest [19–21]. One of the platforms is twisted bilayer graphene [22–34]. The electronic structure of this kind of quasi-two-dimensional system is significantly modified by the Moiré superlattice, leading to almost flat bands.

The nontrivial Berry phase of the flat bands generates large out-of-plane orbital magnetic moment [35–39], which is believed to be relevant to switching in twisted bilayer graphene [40–42]. The orbital moment's effect on light propagating in the plane of a thin structure is fairly straightforward, but for light passing through the plane, the situation is more complex. The quasi-2D chiral structure should give rise to optical gyrotropy on symmetry grounds, with some connection to the in-plane orbital magnetic moment, which still remains obscure due to the breaking of translation symmetry along the out-of-plane direction [43,44].

In this paper, we start from a standard multiband Kubo formula to derive a generic expression for GME current (or equivalently optical rotation) in quasi-2D materials induced by low-frequency light. We show that the orbital magnetic moment can be expressed in terms of the position operator in the presence of open boundary condition. Similar to recent work on nonlinear optical responses with respect to electric field [45,46], we provide a diagrammatic interpretation for the Kubo formula results, which in this case should be viewed as responding to magnetic field. By stacking quasi-2D layers periodically along the out-of-plane direction, one obtains a thermodynamic limit in which the system is equivalent to a 3D bulk material. The relations between the 2D finite layered formula and 3D bulk formula are also discussed, both analytically and numerically. Optical rotation is a powerful and widely used probe of chirality of quasi-2D materials, and we hope that our results will extend this technique from
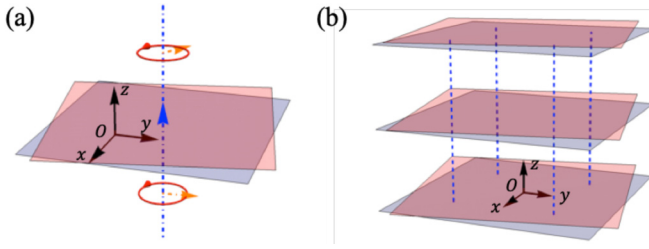
FIG. 1. (a) The rotation of the polarization plane of light passing through a quasi-two-dimensional chiral material (see the blue and red sheets). The blue dashed arrow perpendicular to the plane denotes the direction of the light. The orange arrows show the rotation of the polarization plane. (b) Stacking of quasi-2D layers with chiral structure described in (a), the blue dashed lines illustrate the interlayer couplings.

simply a probe of symmetry, or the sign of twisting, to a more quantitative probe of electronic chirality.

The paper is structured as follows. In Sec. II, we briefly introduce the model Hamiltonian, as well as basic properties of the GME coefficient and optical rotation. In Sec. III, we derive a formula for GME coefficient of quasi-2D material, and show the emergence of the position operator in the low-frequency limit. In Sec. IV, we give a diagrammatic interpretation of a formula derived from Sec. III. In Sec. V, we use the 2D formula to calculate the GME coefficient for periodic stacked many-layer system, and show its convergence to 3D bulk results in thermodynamic limit. We discuss and summarize the main results in Sec. VI, with an eye towards future applications.

II. PRELIMINARIES: HAMILTONIAN AND GME

The rotation of the plane of polarization of light passing through a nonmagnetic material is known as natural optical activity or optical gyrotropy. Consider the optical gyrotropy for chiral quasi-2D materials on x-y plane. Here the term quasi-2D means that the system is infinite in the (x, y) plane with well-defined (k_x, k_y), while maintaining finite open boundary conditions along the $\hat{z}$ direction, which encodes inhomogeneous structure. Figure 1(a) shows the minimal structure of a single (effectively) chiral layer, which consists of two sheets (see the blue and red planes). On the other hand, one can stack and couple N_z copies of structure mentioned in Fig. 1(a) along the $\hat{z}$ direction, making a 3D bulk chiral material in the thermodynamic limit, as shown in Fig. 1(b). For such materials, optical rotation at low frequencies has been shown to be related to the orbital magnetic moment of 3D Bloch electrons on the Fermi surface [3,8].

A. Model

Let us first consider the following Pauli Hamiltonian for a free fermion with spin-orbit coupling [3,47], which will be the starting point for either of the aforementioned cases (single-layer or many-layer slabs):

$$\mathcal{H}_0 = \frac{\mathbf{p}^2}{2m} + V(\mathbf{r}) + \frac{\hbar}{4m^2c^2}(\mathbf{p} \cdot \boldsymbol{\sigma}) \times \nabla V(\mathbf{r}), \quad (1)$$

with m the electron mass, $\mathbf{p}$ the electron momenta, c the speed of light, $\boldsymbol{\sigma} = (\sigma_x, \sigma_y, \sigma_z)$ the Pauli matrices, and $V(\mathbf{r})$ the lattice potential. Here and after we set $c = 1$ for simplicity. The kinematic momentum associated with $\mathcal{H}_0$ is then defined as:

$$\hat{\boldsymbol{\pi}} = \frac{m}{i\hbar}[\hat{\mathbf{r}}, \mathcal{H}_0] = \hat{\mathbf{p}} + \frac{\hbar}{4m}\boldsymbol{\sigma} \times \nabla V(\mathbf{r}), \quad (2)$$

which satisfies the commutation relation $[\hat{r}_i, \hat{\pi}_j] = [\hat{r}_i, \hat{p}_j] = i\hbar\delta_{ij}$. To the leading order of vector potential $\mathbf{A}(\mathbf{r}, t) = \mathbf{A}(\omega, \mathbf{q})e^{i\mathbf{q}\cdot\mathbf{r}-i\omega t}$, with $\mathbf{q} = (q_x, q_y, q_z)$, the coupling with an external electromagnetic field can be treated as a perturbation:

$$\mathcal{H}_I \approx \frac{e}{2}[\hat{\mathbf{v}} \cdot \mathbf{A}(\mathbf{r}, t) + \mathbf{A}(\mathbf{r}, t) \cdot \hat{\mathbf{v}}] + \frac{g_s e}{2m}[\nabla \times \mathbf{A}(\mathbf{r}, t)] \cdot \mathbf{S}, \quad (3)$$

with $\mathbf{S} = (\hbar/2)\boldsymbol{\sigma}$ being the spin operator. Here the $\hat{\mathbf{v}} = \hat{\boldsymbol{\pi}}/m$ is the velocity operator without the external field, whose Fourier transformation is defined as: $\boldsymbol{\pi}_{\mathbf{q}} = e^{-i\mathbf{q}\cdot\mathbf{r}}\hat{\boldsymbol{\pi}}e^{+i\mathbf{q}\cdot\mathbf{r}}$. Thus the total Hamiltonian reads:

$$\mathcal{H} = \mathcal{H}_0 + \mathcal{H}_I. \quad (4)$$

The velocity operator in the presence of electromagnetic fields can be defined as follows:

$$\hat{\mathbf{v}}^{\text{tot}} = \frac{1}{i\hbar}[\mathbf{r}, \mathcal{H}] = \frac{\hat{\boldsymbol{\pi}}}{m} + \frac{e\mathbf{A}(\mathbf{r}, t)}{m}. \quad (5)$$

One can transform the Hamiltonian $\mathcal{H}_0$ into Fourier space $H_0(k_x, k_y)$, whose eigenstates $|\Psi_{\mathbf{k}}^j\rangle = |\Psi_{k_x,k_y}^j\rangle = \mathcal{V}^{-1/2}e^{ik_x x + ik_y y}|u_{k_x,k_y}^j(z)\rangle$, i.e., the 2D Bloch states satisfy $H_0(k_x, k_y)|\Psi_{k_x,k_y}^j\rangle = E_{k_x,k_y}^j|\Psi_{k_x,k_y}^j\rangle$. The Bloch states are normalized for the entire volume $\mathcal{V}$ of the 3D slab: $\langle\Psi_{\mathbf{k}}^m|\Psi_{\mathbf{k}'}^n\rangle_{\text{All}} = \delta_{mn}\delta_{\mathbf{k},\mathbf{k}'}$. Note that j is the band index, which mixes the spin, orbital, and sheet/layer structure encoded along $\hat{z}$ direction.

Now let us assume that in tight-binding limit the Hamiltonian is expanded under maximally localized Wannier functions $|\phi_s^j\rangle$, which can diagonalize the position operator $\hat{z}|\phi_s^j\rangle = (R_s + r_j)|\phi_s^j\rangle$. Here s labels the unit cell and j labels the generalized orbital within the unit cell. R_s denotes the z position for the center of sth unit cell, while r_j is the z position for the center of orbital with respect to the center of the unit cell. The Bloch-like basis reads: $|\chi_k^j\rangle = \sum_s e^{ik(R_s+r_j)}|\phi_s^j\rangle$, and the Bloch states can be expanded as: $|\Psi_{\mathbf{k}}^n\rangle = \mathcal{V}^{-1/2}\sum_j C_{\mathbf{k},j}^n|\chi_{\mathbf{k}}^j\rangle$. We note that here we excluded certain topologically nontrivial states such as Chern insulators for which not all states can be localized.

B. GME coefficient

In this section, we briefly introduce some concepts and notations from the gyrotropic magnetic effect [3,48,49]. Note that, to linear order, the total current density induced by a monochromatic light wave reads:

$$j_i(\mathbf{q}) = \Pi_{ij}(\mathbf{q})A_j(\mathbf{q}) \quad (6)$$

and optical gyrotropy is described by the antisymmetric part of the response tensor $\Pi_{ij}^A = (\Pi_{ij} - \Pi_{ji})/2$ to the order $O(\mathbf{q})$ [1,3]. Its Taylor expansion to first order in $\mathbf{q}$ captures the

natural gyrotropy:

$$\Pi_{ij}^A(\mathbf{q}) = \Pi_{ij}^A(0) + \Pi_{ijl}^A q_l + \cdots . \tag{7}$$

The time-reversal-even part Π_{ijl}^A (GME tensor) with nine independent components is antisymmetric under $i \leftrightarrow j$ and can be written using the GME coefficient α_{ij}^{GME}, where the latter is a rank-two tensor: [3,48,49]

$$\Pi_{ijl}^A = i\epsilon_{ilp}\alpha_{jp}^{\text{GME}} - i\epsilon_{jlp}\alpha_{ip}^{\text{GME}} \tag{8a}$$

$$\alpha_{ij}^{\text{GME}} = \frac{1}{4i}\epsilon_{jlp}(\Pi_{lpi}^A - 2\Pi_{ilp}^A). \tag{8b}$$

In the low-frequency limit $\hbar\omega \ll E_{\text{gap}}$ (E_{gap} stands for the band gap) where only the intraband absorption can occur, we further have:

$$j_i = \alpha_{ij}^{\text{GME}} B_j. \tag{9}$$

For a metal with cubic symmetry or higher, one can derive $\Pi_{ijl}^A = -2i\bar{\alpha}^{\text{GME}}\epsilon_{ijl}$ and $\alpha_{ij}^{\text{GME}} = \bar{\alpha}^{\text{GME}}\delta_{ij}$. With this the rotatory power ρ can be expressed in terms of $\boldsymbol{\alpha}^{\text{GME}}$ [3,4]:

$$\rho = -(1/\epsilon_0)\text{Re}\bar{\alpha}^{\text{GME}}. \tag{10}$$

In general the rotatory power has the unit of rad/unit length. According to Eq. (8b), α_{xx}^{GME} can be expanded by Π_{ijl}^A:

$$\alpha_{xx,2D}^{\text{GME}} = -\frac{i}{2}\Pi_{yzx}^A + \frac{i}{2}\Pi_{xyz}^A - \frac{i}{2}\Pi_{xzy}^A, \tag{11}$$

where those GME tensors can be derived from the standard perturbation theory. One thing we wish to recall for clarity is that the quasi-2D material here still lives in three dimensions, and the only fundamental difference is the breaking of translation symmetry along the out-of-plane direction. The $\alpha_{xx,2D}^{\text{GME}}$ we defined here has the same units compared with the $\alpha_{xx,3D}^{\text{GME}}$ for 3D bulk material, aside from the unit length along the third direction being switched to the thickness of the slab. For example, the rotatory power for a 3D bulk material by stacking infinite many structures plotted in Fig. 1(a) has the units of rad/a, with a is the lattice constant along $\hat{e}_z$ direction. On the other hand, the rotatory power for a quasi-2D slab with three unit layers shown in Fig. 1(b) has more naturally the units of rad/$3a$ since there is no true unit cell or periodicity along $\hat{e}_z$. The main goal for this paper is to calculate $\alpha_{xx,2D}^{\text{GME}}$ (or $\alpha_{yy,2D}^{\text{GME}}$) for a quasi-2D system, which characterizes the rotation of the polarization plane of light perpendicular to the quasi-2D slab.

III. GENERIC KUBO FORMULA

Based on standard perturbation theory, we first derive the generic 2D formula for antisymmetric conductance tensor $\Pi_{\alpha\beta}^A$ as a function of wave vector of light in Sec. III A. Then, in Sec. III B and Sec. III C, at low-frequency limit we evaluate the GME tensor Π_{xyz}^A and Π_{yzx}^A/Π_{xzy}^A in terms of position operator $\hat{z}$. We derive the α_{xx}^{GME} [Eq. (31)] for 2D material at the end of the section, which is the main general result of this paper.

A. Response tensor for 2D material

We start this section from standard perturbation theory. We first derive the net current, then we treat the electromagnetic

field as the perturbation, and evaluate the perturbative matrix element restricted by photon-momenta transfer. Finally we arrive at the main result of this section, which is the rank-2 antisymmetric conductance tensor $\Pi_{\alpha\beta}^A$, see in Eq. (21).

1. Net current

Based on standard perturbation theory [50–53], the 2D current density induced by the monochromatic light $\mathbf{A}(\mathbf{r}, t) = \mathbf{A}(\omega, \mathbf{q})e^{i\mathbf{q}\cdot\mathbf{r} - i\omega t}$ reads:

$$\hat{J}(\mathbf{q}) = -\frac{e}{2}\text{Tr}\big[(\hat{\mathbf{v}}^{\text{tot}}e^{-i\mathbf{q}\cdot\mathbf{r}} + e^{-i\mathbf{q}\cdot\mathbf{r}}\hat{\mathbf{v}}^{\text{tot}})\mathcal{N}\big]$$

$$\approx -\frac{e^2}{m}\text{Tr}\big[e^{-i\mathbf{q}\cdot\mathbf{r}}\mathcal{N}_0\mathbf{A}(\mathbf{r}, t)\big]$$

$$-\frac{e}{2}\text{Tr}\big[(\hat{\mathbf{v}}e^{-i\mathbf{q}\cdot\mathbf{r}} + e^{-i\mathbf{q}\cdot\mathbf{r}}\hat{\mathbf{v}})\delta\mathcal{N}\big], \tag{12}$$

where the trace and integral is conducted in "All" space $\mathcal{V}$ under the quasi-2D Bloch states $|\Psi_{\mathbf{k}}^j\rangle$ defined in Sec. II A. Here the particle density $\mathcal{N}$ has been decomposed into the unperturbed density $\mathcal{N}_0$ and the density fluctuation induced by interaction: $\mathcal{N} = \mathcal{N}_0 + \delta\mathcal{N}$.

One can also decompose the total current Eq. (12) as $\hat{J}(\mathbf{q}) = \hat{J}^1(\mathbf{q}) + \hat{J}^2(\mathbf{q})$. The first term $\hat{J}^1(\mathbf{q})$ is the so-called diamagnetic term:

$$\hat{J}^1(\mathbf{q}) = -\frac{e^2}{m}\text{Tr}\big[e^{-i\mathbf{q}\cdot\mathbf{r}}\mathcal{N}_0\mathbf{A}(\mathbf{r}, t)\big] = -\frac{e^2}{m}\sum_j f(E_j)\mathbf{A}, \tag{13}$$

where $f(E_j) = 1/(1 + e^{(E_j-\mu)/k_BT})$ is the Fermi distribution function for the system with chemical potential μ. Hereafter, we simply write $\mathbf{A}$ for $\mathbf{A}(\omega, \mathbf{q})$.

Now we want to evaluate the second term in Eq. (12):

$$\hat{J}^2(\mathbf{q}) = -\frac{e}{2}\text{Tr}\big[(\hat{\mathbf{v}}e^{-i\mathbf{q}\cdot\mathbf{r}} + e^{-i\mathbf{q}\cdot\mathbf{r}}\hat{\mathbf{v}})\delta\mathcal{N}\big]. \tag{14}$$

We insert a complete set $\mathbb{1} = \sum_{\mathbf{k}',j'}|\Psi_{\mathbf{k}'}^{j'}\rangle\langle\Psi_{\mathbf{k}'}^{j'}|$ inside: $\hat{J}^2(\mathbf{q}) = -\frac{e}{2}\sum_{j,j'}\sum_{\mathbf{k}',\mathbf{k}}\langle\Psi_{\mathbf{k}}^j|(\hat{\mathbf{v}}e^{-i\mathbf{q}\cdot\mathbf{r}} + e^{-i\mathbf{q}\cdot\mathbf{r}}\hat{\mathbf{v}})|\Psi_{\mathbf{k}'}^{j'}\rangle\langle\Psi_{\mathbf{k}'}^{j'}|\delta\mathcal{N}|\Psi_{\mathbf{k}}^j\rangle$. We will consider the $\langle\Psi_{\mathbf{k}}^j|(\hat{\mathbf{v}}e^{-i\mathbf{q}\cdot\mathbf{r}} + e^{-i\mathbf{q}\cdot\mathbf{r}}\hat{\mathbf{v}})|\Psi_{\mathbf{k}'}^{j'}\rangle$ in Sec. III A 2.

The matrix element $\langle\Psi_{\mathbf{k}'}^{j'}|\delta\mathcal{N}|\Psi_{\mathbf{k}}^j\rangle$ can be derived from Schrodinger equation under adiabatic approximation [3,51,54], with $\eta = 1/\tau$ interpreted as the scattering rate:

$$\langle\Psi_{\mathbf{k}'}^{j'}|\delta\mathcal{N}|\Psi_{\mathbf{k}}^j\rangle = \frac{f^0(E_{\mathbf{k}'}^{j'}) - f^0(E_{\mathbf{k}}^j)}{E_{\mathbf{k}'}^{j'} - E_{\mathbf{k}}^j - \hbar\omega - i\hbar\eta}\langle\Psi_{\mathbf{k}'}^{j'}|\mathcal{H}_I|\Psi_{\mathbf{k}}^j\rangle, \tag{15}$$

Following some well-known tricks in the low-frequency limit [3,54], we find that the prefactor $[f^0(E_{\mathbf{k}'}^{j'}) - f^0(E_{\mathbf{k}}^j)]/(E_{\mathbf{k}'}^{j'} - E_{\mathbf{k}}^j - \hbar\omega - i\hbar\eta)$ can be divided into two parts:

$$\frac{\hbar\omega[f^0(E_{\mathbf{k}}^j) - f^0(E_{\mathbf{k}'}^{j'})]}{E_{\mathbf{k}}^j - E_{\mathbf{k}'}^{j'} + i\hbar\eta}\left(\frac{1}{\hbar\omega} - \frac{1}{\hbar\omega + E_{\mathbf{k}}^j - E_{\mathbf{k}'}^{j'}}\right). \tag{16}$$

The first term in Eq. (16) can be viewed as: $\mathcal{P}\{[f^0(E_{\mathbf{k}}^j) - f^0(E_{\mathbf{k}'}^{j'})]/(E_{\mathbf{k}}^j - E_{\mathbf{k}'}^{j'})\} + i\pi[f^0(E_{\mathbf{k}}^j) - f^0(E_{\mathbf{k}'}^{j'})]\delta(E_{\mathbf{k}}^j - E_{\mathbf{k}'}^{j'})$, where the $\mathcal{P}$ stands for Cauchy principle value. The term related to principle value canceled with the diamagnetic term $\hat{J}^1(\mathbf{q})$ [Eq. (13)]. The second term vanishes, since when

$\delta(E_{\mathbf{k}}^j - E_{\mathbf{k}'}^{j'}) = 1$, we have $f^0(E_{\mathbf{k}}^j) - f^0(E_{\mathbf{k}'}^{j'}) = 0$ [3,54]. Thus, by combining $\hat{J}^1(\mathbf{q})$ and $\hat{J}^2(\mathbf{q})$, only the second term of Eq. (16) contributes to the net current:

$$\hat{J}(\mathbf{q}) = -\frac{e}{2} \sum_{j,j'} \sum_{\mathbf{k}',\mathbf{k}} \langle \Psi_{\mathbf{k}}^j | [\hat{v}e^{-i\mathbf{q}\cdot\mathbf{r}} + e^{-i\mathbf{q}\cdot\mathbf{r}}\hat{v}] | \Psi_{\mathbf{k}'}^{j'} \rangle \langle \delta\mathcal{N} \rangle_{\mathbf{k}'\mathbf{k}}^{j'j}.$$
(17)

Here we define $\langle \delta\mathcal{N} \rangle_{\mathbf{k}'\mathbf{k}}^{j'j} = F_{\mathbf{k},\mathbf{k}'}^{jj'} \langle \Psi_{\mathbf{k}'}^{j'} | \mathcal{H}_{\mathrm{I}} | \Psi_{\mathbf{k}}^j \rangle$, with

$$F_{\mathbf{k}\mathbf{k}'}^{jj'} = -\frac{f^0(E_{\mathbf{k}}^j) - f^0(E_{\mathbf{k}'}^{j'})}{E_{\mathbf{k}}^j - E_{\mathbf{k}'}^{j'} + i\hbar\eta} \frac{\hbar\omega}{\hbar\omega + E_{\mathbf{k}}^j - E_{\mathbf{k}'}^{j'} + i\hbar\eta}. \quad (18)$$

2. Perturbative matrix element and momentum transfer

We would like to evaluate the matrix element of $\mathcal{H}_{\mathrm{I}}$ between two Bloch states. For the monochromatic light with wave vector $\mathbf{q} = (\tilde{\mathbf{q}}, q_z) = (q_x, q_y, q_z)$, and vector potential $\mathbf{A} = (A_x, A_y, A_z)$, we have the coupling with light as:

$$\mathcal{H}_{\mathrm{I}} = \frac{e}{2} \sum_i [v_i e^{i(q_x x + q_y y + q_z z)} + e^{i(q_x x + q_y y + q_z z)} v_i] A_i. \quad (19)$$

Note that, in a quasi-2D layered system (a slab in $\hat{z}$ direction), for given cell-periodic operator $\hat{\mathcal{O}}_{\mathbf{k}} = e^{-i\mathbf{k}\cdot\mathbf{r}}\hat{\mathcal{O}}e^{+i\mathbf{k}\cdot\mathbf{r}}$ (say velocity operator $\hat{\mathbf{v}}_{\mathbf{k}}$) we have:

$$\langle \Psi_{\mathbf{k}'}^{j'} | \hat{\mathcal{O}}e^{i\tilde{\mathbf{q}}\cdot\mathbf{r}} | \Psi_{\mathbf{k}}^j \rangle_{\mathrm{All}} = \delta_{k_x, k_x' - q_x} \delta_{k_y, k_y' - q_y} \langle u_{\mathbf{k}'}^{j'} | \hat{\mathcal{O}}_{\mathbf{k}'} | u_{\mathbf{k}}^j \rangle_{\mathrm{Cell}}. \quad (20)$$

Here "All" stands for the entire space $\mathcal{V}$ where the Bloch states is defined, while the "Cell" stands for the volume of a quasi-2D unit cell. By applying this relation, i.e., take $\hat{\mathcal{O}} = \hat{\mathbf{v}}e^{iq_z z}$, which is cell periodic in (x, y) plane, then we will see: $\langle \Psi_{\mathbf{k}'}^{j'} | \mathcal{H}_{\mathrm{I}} | \Psi_{\mathbf{k}}^j \rangle_{\mathrm{All}} = \delta_{\mathbf{k},\mathbf{k}'-\tilde{\mathbf{q}}} \langle u_{\mathbf{k}+\tilde{\mathbf{q}}}^{j'} | \mathcal{H}_{\mathrm{I},\mathbf{k}+\tilde{\mathbf{q}}/2} | u_{\mathbf{k}}^j \rangle_{\mathrm{Cell}}$, where $\mathcal{H}_{\mathrm{I},\mathbf{k}+\tilde{\mathbf{q}}/2,\beta}$ stands for the 2D Fourier transformation of the term associated with A_β in Eq. (19). Here $\mathcal{H}_{\mathrm{I},\mathbf{k}+\tilde{\mathbf{q}}/2,\beta}$ stands for the 2D Fourier transformation of the term associated with A_β in Eq. (19). Similar tricks also apply for the matrix element ahead of $\langle \delta\mathcal{N} \rangle_{\mathbf{k}'\mathbf{k}}^{j'j}$ in Eq. (17): $\langle \Psi_{\mathbf{k}}^j | (\hat{v}e^{-i\mathbf{q}\cdot\mathbf{r}} + e^{-i\mathbf{q}\cdot\mathbf{r}}\hat{v}) | \Psi_{\mathbf{k}'}^{j'} \rangle_{\mathrm{All}} = \langle u_{\mathbf{k}}^j | v_{\mathbf{k}+\tilde{\mathbf{q}}/2,\alpha} e^{-iq_z r_z} + e^{-iq_z r_z} v_{\mathbf{k}+\tilde{\mathbf{q}}/2,\alpha} | u_{\mathbf{k}+\tilde{\mathbf{q}}}^{j'} \rangle_{\mathrm{Cell}}$. Now we have successfully transformed the full space integral into the cell integral, and illustrated the momentum shift restriction for a quasi-2D Bloch electron's scattering with light.

3. Rank-2 GME tensor $\Pi_{\alpha\beta}^A$

Combined with results in Sec. III A 2, one can subtract the conductance tensor $j_\alpha = \Pi_{\alpha\beta} A_\beta$ from Eq. (17). The GME tensor is related to its antisymmetric part $\Pi_{\alpha\beta}^A = (\Pi_{\alpha\beta} - \Pi_{\beta\alpha})/2$:

$$\Pi_{\alpha\beta}^A = ie \sum_{j,j',\mathbf{k}} F_{\mathbf{k}\mathbf{k}+\tilde{\mathbf{q}}}^{jj'} \mathcal{M}_{\alpha\beta}^A, \quad (21a)$$

$$\mathcal{M}_{\alpha\beta}^A = \mathrm{Im} \langle u_{\mathbf{k}}^j | v_{\mathbf{k}+\tilde{\mathbf{q}}/2,\alpha} e^{-iq_z r_z} + e^{-iq_z r_z} v_{\mathbf{k}+\tilde{\mathbf{q}}/2,\alpha} | u_{\mathbf{k}+\tilde{\mathbf{q}}}^{j'} \rangle$$
$$\times \langle u_{\mathbf{k}+\tilde{\mathbf{q}}}^{j'} | \mathcal{H}_{\mathrm{I},\mathbf{k}+\tilde{\mathbf{q}}/2,\beta} | u_{\mathbf{k}}^j \rangle / 2. \quad (21b)$$

Hereafter we drop the subscript "Cell" ("All") if the operator is evaluated under cell-periodic part of Bloch wave function (full Bloch wave function).

Note that $F_{\mathbf{k}\mathbf{k}+\tilde{\mathbf{q}}}^{jj'}$ does not explicitly depend on q_z. One can send $\tilde{\mathbf{q}} \to 0$. In this case $\mathbf{k}' \to \mathbf{k}$. We have assumed that the frequency is so low, such that $\forall \mathbf{k} = (k_x, k_y), j \neq j'$, $|E_{\mathbf{k}}^j - E_{\mathbf{k}}^{j'}| \gg \hbar\omega$, thus $F_{\mathbf{k},\mathbf{k}+\tilde{\mathbf{q}}}^{jj'} = 0$. For the $j = j'$, we will see:

$$F_{\mathbf{k}}^{jj'} = \lim_{\tilde{\mathbf{q}} \to 0} F_{\mathbf{k}\mathbf{k}+\tilde{\mathbf{q}}}^{jj'} = -\lim_{\tilde{\mathbf{q}} \to 0} \frac{f^0(E_{\mathbf{k}}^j) - f^0(E_{\mathbf{k}+\tilde{\mathbf{q}}}^j)}{E_{\mathbf{k}}^j - E_{\mathbf{k}+\tilde{\mathbf{q}}}^j} \frac{\hbar\omega}{\hbar\omega + i\hbar\eta}$$

$$= -\frac{\partial f^0(E_{\mathbf{k}}^j)}{\partial E_{\mathbf{k}}^j} \frac{\hbar\omega}{\hbar\omega + i\hbar\eta} = \frac{\partial f^0(E_{\mathbf{k}}^j)}{\partial E_{\mathbf{k}}^j} \frac{i\omega\tau}{1 - i\omega\tau}, \quad (22)$$

where we have interpreted $\eta = 1/\tau$ as a scattering rate $1/\tau$ [3,54]. In this case $\Pi_{\alpha\beta}^A$ reads:

$$\Pi_{\alpha\beta}^A = \frac{e^2\omega\tau}{1 - i\omega\tau} \sum_j \sum_{\mathbf{k}} \frac{\partial f^0(E_{\mathbf{k}}^j)}{\partial E_{\mathbf{k}}^j} \mathcal{M}_{\alpha\beta}^A, \quad (23)$$

with $\mathcal{M}_{\alpha\beta}^A$ given in Eq. (21) for $j = j'$.

B. GME tensor Π_{xyz}^A

To get Π_{xyz}^A, let us assume that we have light that is not strictly perpendicular to the (x, y) plane. Instead, assuming that $\mathbf{q} = (q_x, 0, q_z)$, i.e., $\tilde{\mathbf{q}} = (q_x, 0)$ with $|\tilde{\mathbf{q}}| \ll |q_z|$. We can approximately view $\mathbf{A} = (0, A_y, 0)$. In this case we will have $\mathbf{q} \cdot \mathbf{r} = q_x x + q_z z$. The coupling with light reads: $\mathcal{H}_{\mathrm{I}} = \frac{e}{2}[v_y e^{i(q_x x + q_z z)} + e^{i(q_x x + q_z z)} v_y] A_y$. Substituting back to Eq. (21) we have: $\mathcal{M}_{xy}^A(q_z) = \mathrm{Im}[\langle u_{\mathbf{k}}^j | \hat{v}_{\mathbf{k}+\tilde{\mathbf{q}}/2,x} e^{-iq_z z} | u_{\mathbf{k}+\tilde{\mathbf{q}}}^j \rangle \langle u_{\mathbf{k}+\tilde{\mathbf{q}}}^j | \hat{v}_{\mathbf{k}+\tilde{\mathbf{q}}/2,y} e^{+iq_z z} | u_{\mathbf{k}}^j \rangle]$. We first take the low-frequency limit, and then send $\tilde{\mathbf{q}} \to 0$, such that $F_{\mathbf{k}}^{j'j} = F_{\mathbf{k}}^{jj} \delta_{j'j} = \delta_{j'j} [\partial f^0(E_{\mathbf{k}}^j)/\partial E_{\mathbf{k}}^j][i\omega\tau/(1 - i\omega\tau)]$. With above we have the conductance tensor as:

$$\Pi_{xy}^A = \frac{e^2\omega\tau}{1 - i\omega\tau} \sum_j \sum_{\mathbf{k}} \frac{\partial f^0(E_{\mathbf{k}}^j)}{\partial E_{\mathbf{k}}^j} \mathcal{M}_{xy}^A(q_z), \quad (24a)$$

$$\mathcal{M}_{xy}^A(q_z) = \mathrm{Im} \langle u_{\mathbf{k}}^j | \hat{v}_{\mathbf{k},x} e^{-iq_z z} | u_{\mathbf{k}}^j \rangle \langle u_{\mathbf{k}}^j | \hat{v}_{\mathbf{k},y} e^{+iq_z z} | u_{\mathbf{k}}^j \rangle. \quad (24b)$$

Here $\hat{v}_{\mathbf{k},x} = \hbar^{-1} \partial_{k_x} H_0(k_x, k_y)$, and $\hat{v}_{\mathbf{k},y} = \hbar^{-1} \partial_{k_y} H_0(k_x, k_y)$. Note that in Eq. (23) we have used the fact that $\hat{v}_{\mathbf{k},x}$ and $\hat{v}_{\mathbf{k},y}$ does not explicitly contain z, such that they commute with $e^{\pm iq_z z}$. We would like to evaluate Eq. (23) to the leading order of q_z. One can carry out the Taylor expansion as follows: $e^{\pm iq_z z} \approx 1 \pm iq_z z$ in small q_z limit, drop the real part $\langle u_{\mathbf{k}}^j | \hat{v}_{\mathbf{k},x} | u_{\mathbf{k}}^j \rangle \langle u_{\mathbf{k}}^j | \hat{v}_{\mathbf{k},y} | u_{\mathbf{k}}^j \rangle$, and insert a complete set between $\hat{v}_{\mathbf{k},y}$ and $\hat{z}$, such that we have

$$\mathcal{M}_{xyz}^A \approx \sum_{j_1, j_1 \neq j} \mathrm{Re}\big[\langle u_{\mathbf{k}}^j | \hat{v}_{\mathbf{k},x} | u_{\mathbf{k}}^j \rangle \langle u_{\mathbf{k}}^j | \hat{v}_{\mathbf{k},y} | u_{\mathbf{k}}^{j_1} \rangle \langle u_{\mathbf{k}}^{j_1} | \hat{z} | u_{\mathbf{k}}^j \rangle$$
$$- \langle u_{\mathbf{k}}^j | \hat{v}_{\mathbf{k},x} | u_{\mathbf{k}}^{j_1} \rangle \langle u_{\mathbf{k}}^{j_1} | \hat{z} | u_{\mathbf{k}}^j \rangle \langle u_{\mathbf{k}}^j | \hat{v}_{\mathbf{k},y} | u_{\mathbf{k}}^j \rangle \big], \quad (25)$$

with the $j_1 = j$ term canceling out.

C. GME tensor Π_{yzx}^A and Π_{xzy}^A.

The calculation of $\Pi_{\alpha z\beta}^A$ [with $(\alpha, \beta) = (x, y)$ or (y, x)] is slightly different from Π_{xyz}^A due to the lack of periodicity in z direction. Let us assume the light with wave vector $\mathbf{q}$, while $\tilde{\mathbf{q}} = q_\beta \hat{e}_\beta$, $q_z = 0$, and $\mathbf{A} = (0, 0, A_z)$. Accordingly,

the coupling with light reads: $\mathcal{H}_I = \frac{e}{2}(v_z e^{iq_\beta v_\beta} + e^{iq_\beta v_\beta} v_z)A_z$. Similar to the calculation in Π^A_{xyz}, by using Eq. (23), in the low-frequency limit we have:

$$\mathcal{M}^A_{\alpha z}(q_\beta) = \mathrm{Im}\big[\langle u^j_{\mathbf{k}}|\, \hat{v}_{\mathbf{k}+q_\beta \hat{e}_\beta/2,\alpha}\, |u^j_{\mathbf{k}'}\rangle\langle u^j_{\mathbf{k}'}|\, \hat{v}_z\, |u^j_{\mathbf{k}}\rangle\big], \qquad (26)$$

with $\mathbf{k}' = \mathbf{k} + q_\beta \hat{e}_\beta$. Here $\hat{v}_{\mathbf{k},\alpha} = \hbar^{-1}\partial_{k_\alpha} H_0(k_x, k_y)$ and $\hat{\mathbf{v}}_{\mathbf{k}\pm\mathbf{q}/2} = \hat{\mathbf{v}}_{\mathbf{k}} \pm \mathbf{q}/2m$ [47] for $\alpha = x, y$. However, $\hat{v}_z$ can not be written in this form due to the breaking of translation symmetry along $\hat{e}_z$ direction, one can treat $\hat{v}_z$ as in real space since it commutes with $e^{i\mathbf{k}\cdot\mathbf{r}}$ and $e^{iq_\beta v_\beta}$. With the above we can expand $|u^j_{\mathbf{k}}\rangle$ and $\langle u^j_{\mathbf{k}}|$ to the leading order of q_β ($|u^j_{\mathbf{k}+q_\beta \hat{e}_\beta}\rangle \approx |u^j_{\mathbf{k}}\rangle + |\partial_{k_\beta} u^j_{\mathbf{k}}\rangle q_\beta$ and $\langle u^j_{\mathbf{k}+q_\beta \hat{e}_\beta}| \approx \langle u^j_{\mathbf{k}}| + \langle \partial_{k_\beta} u^j_{\mathbf{k}}|q_\beta$), and substitute back into Eq. (26), we arrive at:

$$\mathcal{M}^A_{\alpha z}(q_\beta) = \mathrm{Im}\big[\langle u^j_{\mathbf{k}}|\, \hat{v}_{\mathbf{k},\alpha}\, |\partial_{k_\beta} u^j_{\mathbf{k}}\rangle\langle u^j_{\mathbf{k}}|\, \hat{v}_z\, |u^j_{\mathbf{k}}\rangle\big]q_\beta$$
$$+ \mathrm{Im}\big[\langle u^j_{\mathbf{k}}|\, \hat{v}_{\mathbf{k},\alpha}\, |u^j_{\mathbf{k}}\rangle\langle \partial_{k_\beta} u^j_{\mathbf{k}}|\, \hat{v}_z\, |u^j_{\mathbf{k}}\rangle\big]q_\beta + O(q^2_\beta), \qquad (27)$$

where we have dropped the real part $\langle u^j_{\mathbf{k}}|\, \hat{v}_{\mathbf{k},\alpha}\, |u^j_{\mathbf{k}}\rangle\langle u^j_{\mathbf{k}}|\, \hat{v}_z\, |u^j_{\mathbf{k}}\rangle$. By inserting a complete set inside we have:

$$\mathcal{M}^A_{\alpha z\beta} = \sum_{j_1, j_1\neq j} \mathrm{Im}\big[\langle u^j_{\mathbf{k}}|\, \hat{v}_{\mathbf{k},\alpha}\, |u^{j_1}_{\mathbf{k}}\rangle\langle u^{j_1}_{\mathbf{k}}|\, \partial_{k_\beta} u^j_{\mathbf{k}}\rangle\langle u^j_{\mathbf{k}}|\, \hat{v}_z\, |u^j_{\mathbf{k}}\rangle$$
$$- \langle u^j_{\mathbf{k}}|\, \hat{v}_{\mathbf{k},\alpha}\, |u^j_{\mathbf{k}}\rangle\langle u^j_{\mathbf{k}}|\, \partial_{k_\beta} u^{j_1}_{\mathbf{k}}\rangle\langle u^{j_1}_{\mathbf{k}}|\, \hat{v}_z\, |u^j_{\mathbf{k}}\rangle\big], \qquad (28)$$

where we have used the fact $\langle u^{j_1}_{\mathbf{k}}|\partial_{k_\beta} u^j_{\mathbf{k}}\rangle = -\langle \partial_{k_\beta} u^{j_1}_{\mathbf{k}}|u^j_{\mathbf{k}}\rangle$ such that the $j_1 = j$ terms cancel out.

Note that, in the presence of open boundary condition or for an infinite system, we have the following relation [47,55,56] standing for $j \neq l$ ($\hat{\mathbf{p}} = im[H, \mathbf{r}]/\hbar$):

$$\langle\hat{v}_z\rangle^{jl}_{\mathbf{k}} = \langle u^j_{\mathbf{k}}|\, \hat{v}_z\, |u^l_{\mathbf{k}}\rangle = i\Omega^{jl}_{\mathbf{k}}\langle u^j_{\mathbf{k}}|\, \hat{z}\, |u^l_{\mathbf{k}}\rangle,$$
$$\langle u^j_{\mathbf{k}}|\partial_{k_\beta} u^l_{\mathbf{k}}\rangle = -\frac{1}{\Omega^{jl}_{\mathbf{k}}}\langle\hat{v}_{\mathbf{k},\beta}\rangle^{jl}_{\mathbf{k}} = -\frac{1}{\Omega^{jl}_{\mathbf{k}}}\langle u^j_{\mathbf{k}}|\, \hat{v}_{\mathbf{k},\beta}\, |u^l_{\mathbf{k}}\rangle \qquad (29)$$

with $\Omega^{jl}_{\mathbf{k}} = \hbar^{-1}(E^j_{\mathbf{k}} - E^l_{\mathbf{k}})$ and the position operator defined trivially as in Sec. II A. For a finite system with periodic boundary conditions, an additional correction term should be taken into consideration or we need to use the quantum position operator [56–58], but this is not a case that we consider in this paper. Substituting Eq. (29) back to Eq. (28) we have:

$$\mathcal{M}^A_{\alpha z\beta} = \sum_{j_1, j_1\neq j} \mathrm{Im}\big[-i\langle\hat{v}_{\mathbf{k},\alpha}\rangle^{jj_1}_{\mathbf{k}}\langle\hat{v}_{\mathbf{k},\beta}\rangle^{jj_1}_{\mathbf{k}}\langle\hat{z}\rangle^{j_1 j}_{\mathbf{k}}$$
$$- \frac{1}{\Omega^{j_1 j}_{\mathbf{k}}}\langle\hat{v}_{\mathbf{k},\alpha}\rangle^{jj_1}_{\mathbf{k}}\langle\hat{v}_{\mathbf{k},\beta}\rangle^{j_1 j}_{\mathbf{k}}\langle\hat{v}_z\rangle^{jj}_{\mathbf{k}}\big]. \qquad (30)$$

Combining Eq. (25), Eq. (30), and Eq. (11), we arrive at the GME coefficient:

$$\alpha^{\mathrm{GME}}_{xx,2D} = \frac{i\omega\tau}{1-i\omega\tau}\sum_{\mathbf{k}}\sum_j \frac{\partial f^0(E^j_{\mathbf{k}})}{\partial E^j_{\mathbf{k}}}\langle\hat{v}_{\mathbf{k},x}\rangle^{jj}_{\mathbf{k}}\sum_{j_1, j_1\neq j}\frac{e^2}{2}\mathrm{Re}\big[\langle\hat{v}_{\mathbf{k},y}\rangle^{jj_1}_{\mathbf{k}}\langle\hat{z}\rangle^{j_1 j}_{\mathbf{k}} + \langle\hat{z}\rangle^{jj_1}_{\mathbf{k}}\langle\hat{v}_{\mathbf{k},y}\rangle^{j_1 j}_{\mathbf{k}}\big]$$
$$= \frac{i\omega\tau}{1-i\omega\tau}\frac{e^2}{2}\sum_{\mathbf{k}}\sum_j \frac{\partial f^0(E^j_{\mathbf{k}})}{\partial E^j_{\mathbf{k}}}\langle\hat{v}_{\mathbf{k},x}\rangle^{jj}_{\mathbf{k}}\mathrm{Re}\big[\langle\hat{v}_{\mathbf{k},y}\hat{z} + \hat{z}\hat{v}_{\mathbf{k},y}\rangle^{jj}_{\mathbf{k}} - 2\langle\hat{z}\rangle^{jj}_{\mathbf{k}}\langle\hat{v}_{\mathbf{k},y}\rangle^{jj}_{\mathbf{k}}\big], \qquad (31)$$

which is the main result of this paper. Note that, due to the orthogonality of eigenstates, the final results do not depend on the chosen zero point of the $\hat{z}$ coordinate. One can shift the origin of $\hat{z}$ coordinates by z_0, such that under new coordinate we have: $\langle u^i_{\mathbf{k}}|\, \hat{z} + z_0 \mathbb{I}_{4N_z\times 4N_z}\, |u^j_{\mathbf{k}}\rangle = \langle u^i_{\mathbf{k}}|\, \hat{z}\, |u^j_{\mathbf{k}}\rangle + z_0\delta_{ij} = \langle u^i_{\mathbf{k}}|\, \hat{z}\, |u^j_{\mathbf{k}}\rangle$, with $i = j$ cases have already been excluded in Eq. (31). Note that the simple form of position operator relies on Eq. (29), which requires no band touching at the Fermi surface.

It may not be obvious at first glance what this result means physically, or how it can be connected to known formulas for the 3D response in terms of the orbital magnetic moment. Hence we next give a diagrammatic explanation for the result, then apply it to slabs of increasing size to see how the 3D limit emerges quantitatively.

IV. DIAGRAMMATIC INTERPRETATION

In this section, similar to recent work on electric dipole responses [45,46], we would like to assign a diagrammatic interpretation for formula Eq. (31). Note that the Hamiltonian

can be written perturbatively as:

$$H(\hbar\mathbf{k} + e\vec{A})$$
$$= \int [d\mathbf{k}]c^\dagger_{\mathbf{k}} H_0(\hbar\mathbf{k})c_{\mathbf{k}} + \int [d\mathbf{k}]c^\dagger_{\mathbf{k}}\left(e\frac{\partial H}{\partial\hbar\mathbf{k}}\cdot\mathbf{A}\right)c_{\mathbf{k}} + \cdots$$
$$= \int [d\mathbf{k}]c^\dagger_{\mathbf{k}} H_0(\hbar\mathbf{k})c_{\mathbf{k}} + \int [d\mathbf{k}]c^\dagger_{\mathbf{k}}(e\hat{\mathbf{v}}\cdot\mathbf{A})c_{\mathbf{k}} + \cdots. \qquad (32)$$

Here $c^\dagger_{\mathbf{k}}$ ($c_{\mathbf{k}}$) stands for the creation (annihilation) operator for a Bloch electron. (Since the speed of light c is much larger than the Fermi velocity $\hat{v}_F$, we only ensure the energy conservation at each vertex [45].) Here $[d\mathbf{k}] = dk_x dk_y/A_{\mathrm{BZ}}$, where A_{BZ} stands for the area of the 2D first Brillouin zone in which the integral is conducted. The first term is the unperturbed Hamiltonian, and the rest of the terms are perturbations from the external electromagnetic field. The amplitude of the diagram tells the response of one vertex (measurement) to the other vertex (perturbation). Let us imagine that we inject the light perpendicular to the x-y plane (along z direction). The magnetic field is in-plane. In Landau gauge $B_x = \nabla \times \mathbf{A}$, where $\mathbf{A} = (0, zB, 0)$. Thus the contribution is from $e\hat{\mathbf{v}}\cdot\mathbf{A}$, and we can write this vertex in the canonical form of position
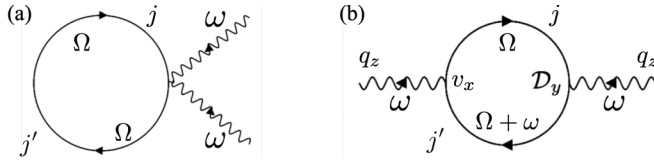
FIG. 2. Two diagrams for Hamiltonian Eq. (32) to the leading order. The solid line and wavy line, denotes, respectively, the electron and photon propagator [45]. (a) The diamagnetic current. (b) The diagram for Eq. (35). The $\mathcal{D}_y$ stands for the vertex for perturbation as defined in Eq. (33) and v_x stands for the vertex for the measurement.

operator as:

$$\mathcal{D}_y = e\hat{\mathbf{v}} \cdot \mathbf{A} = \frac{eB}{2}(\hat{v}_{\mathbf{k},y}\hat{z} + \hat{z}\hat{v}_{\mathbf{k},y}). \tag{33}$$

With the above we can figure out the Feynman diagram for a Bloch electron coupled to external electrical magnetic field, as shown in Fig. 2. The Green's function or the propagator of the electron is defined as [45]:

$$G(\omega) = (\omega - H(\mathbf{k}))^{-1} = \sum_i \frac{|u_{\mathbf{k}}^i\rangle \langle u_{\mathbf{k}}^i|}{\hbar\omega - E_{\mathbf{k}}^i}. \tag{34}$$

The first diagram is the diamagnetic current, same as in Eq. (13). The contribution from the second diagram reads:

$$j_x^{\text{total}} = e\left[\sum_{j'j}\int [d\mathbf{k}]\int d\Omega \langle \hat{v}_{\mathbf{k},x}\rangle_{\mathbf{k}}^{j'j} G_j(\Omega) \langle \mathcal{D}_y\rangle_{\mathbf{k}}^{jj'} G_{j'}(\Omega + \omega)\right]. \tag{35}$$

Note that [45]:

$$I_2 = \int d\Omega\, G_j(\Omega) G_{j'}(\Omega + \omega) = \frac{f^0(E_{\mathbf{k}}^{j'}) - f^0(E_{\mathbf{k}}^j)}{\hbar(\omega + i/\tau) - (E_{\mathbf{k}}^{j'} - E_{\mathbf{k}}^j)}. \tag{36}$$

By using the same trick mentioned in Sec. III, part of I_2 will cancel with the diamagnetic current, while the remaining part contributes to the GME current. In the low-frequency limit, the part we are interested in for I_2 is $\delta_{j'j}\partial f^0(E_{\mathbf{k}}^j)/\partial E_{\mathbf{k}}^j[(i\omega\tau)/(1 - i\omega\tau)]$. We further have the current:

$$j_x^{\text{total}} = \frac{i\omega\tau e}{1 - i\omega\tau}\sum_j \int [d\mathbf{k}]\frac{\partial f^0(E_{\mathbf{k}}^j)}{\partial E_{\mathbf{k}}^j}\langle \hat{v}_{\mathbf{k},x}\rangle_{\mathbf{k}}^{jj}\langle \mathcal{D}_y\rangle_{\mathbf{k}}^{jj}, \tag{37}$$

from which we can subtract the $\alpha_{xx,2D}^{\text{GME}}$ as:

$$\alpha_{xx,2D}^{\text{GME}} = \frac{i\omega\tau}{1 - \omega\tau}\sum_j \int [d\mathbf{k}]\frac{\partial f^0(E_{\mathbf{k}}^j)}{\partial E_{\mathbf{k}}^j}\langle \hat{v}_{\mathbf{k},x}\rangle_{\mathbf{k}}^{jj}$$
$$\times \sum_{j_1}\frac{e^2}{2}\big[\langle \hat{v}_{\mathbf{k},y}\rangle_{\mathbf{k}}^{jj_1}\langle \hat{z}\rangle_{\mathbf{k}}^{j_1j} + \langle \hat{z}\rangle_{\mathbf{k}}^{jj_1}\langle \hat{v}_{\mathbf{k},y}\rangle_{\mathbf{k}}^{j_1j}\big], \tag{38}$$

which is equivalent to Eq. (31), aside from containing the $j = j_1$ term. Note that the terms within the brackets are already real. The result above corresponds to the total current, but the GME is related to its antisymmetric part, so we need to drop the $j = j_1$ since it is invariant under $v_x \leftrightarrow v_y$. This is a

straightforward way to understand the result from the Kubo formula without going through a rigorous calculation.

V. CONNECTION WITH 3D BULK RESULTS IN THERMODYNAMIC LIMIT

Let us consider a stack of N_z layers of the quasi-2D chiral structure along the $\hat{e}_z$ direction, as shown in Fig. 1(b). In the thermodynamic limit, i.e., $N_z \to \infty$, we should have Eq. (31) converging to 3D bulk results [3,8]:

$$\alpha_{xx,3D}^{\text{GME}} = \frac{i\omega\tau e}{(1 - i\omega\tau)}\sum_n \int [dk]\frac{\partial f^0(E_k^n)}{\partial E_k^n}\hat{v}_{k,x}\hat{\mathbf{m}}_{kn,x}, \tag{39a}$$

$$\hat{\mathbf{m}}_{kn} = \frac{e}{2\hbar}\text{Im}\langle \partial_k u_k^n| \times (H_k - E_k^n)|\partial_k u_k^n\rangle, \tag{39b}$$

with $k = (\mathbf{k}, k_z) = (k_x, k_y, k_z)$, $[dk] = dk_x dk_y dk_z/V_{\text{BZ}}$, where V_{BZ} stands for the volume of the 3D first Brillouin zone in which the integral is conducted. We write $|u_k^n\rangle$ for the 3D cell-periodic part of Bloch states, which are the eigenstates of the Bloch Hamiltonian $H_k|u_k^n\rangle = E_k^n|u_k^n\rangle$. By applying Eq. (29) to Eq. (39b) we obtain the orbital magnetic moment written in terms of velocity operators:

$$\hat{\mathbf{m}}_{kn,x} = e\hbar \sum_{m,m\neq n}\text{Im}\left[\frac{\langle u_k^n|\hat{v}_{k,y}|u_k^m\rangle \langle u_k^m|\hat{v}_{k,z}|u_k^n\rangle}{E_k^m - E_k^n}\right]. \tag{40}$$

Before going to realistic models, we provide a straightforward way to understand the connection between the 2D result Eq. (31) and the 3D result Eq. (39a). Applying Eq. (29) along $\hat{e}_z$ direction, we have: $\hbar\langle \hat{v}_{k,y}\rangle_k^{mn} \equiv \langle u_k^m|\hbar\hat{v}_{k,y}|u_k^n\rangle_{\text{Cell}} = \langle u_k^m|\partial_{k_z}H_k|u_k^n\rangle_{\text{Cell}} = i(E_k^m - E_k^n)\langle u_k^m|\hat{z}|u_k^n\rangle_{\text{INV}} \equiv i(E_k^m - E_k^n)\langle \hat{z}\rangle_k^{mn}$, with the subscript INV standing for 3D bulk material with infinite volume. Note that such a replacement is only valid for a 3D bulk material where an infinite integral is conducted [56]. Substituting this to Eq. (40) we have:

$$\hat{\mathbf{m}}_{kn,x} = \frac{e}{2}\sum_{m,m\neq n}\text{Re}\big[\langle \hat{v}_{k,y}\rangle_k^{nm}\langle \hat{z}\rangle_k^{mn} + \langle \hat{z}\rangle_k^{nm}\langle \hat{v}_{k,y}\rangle_k^{mn}\big], \tag{41}$$

with Eq. (41) back to the $\alpha_{xx,3D}^{\text{GME}}$ in Eq. (39a). Finally we arrive at the 3D bulk formula in terms of position operator:

$$\alpha_{xx,3D}^{\text{INV}} = \frac{i\omega\tau}{1 - i\omega\tau}\sum_n \int [dk]\frac{\partial f^0(E_k^n)}{\partial E_k^n}\langle \hat{v}_{k,x}\rangle_k^{nn}\frac{e^2}{2}$$
$$\times \sum_{m,m\neq n}\text{Re}\big[\langle \hat{v}_{k,y}\rangle_k^{nm}\langle \hat{z}\rangle_k^{mn} + \langle \hat{z}\rangle_k^{nm}\langle \hat{v}_{k,y}\rangle_k^{mn}\big], \tag{42}$$

which looks similar to Eq. (31).

From Eq. (31) one can define two relevant variables:

$$\alpha_{xx,2D}^{\text{OBC}}(N_z) = \frac{1}{N_z}\alpha_{xx,2D}^{\text{GME}}(N_z), \tag{43a}$$

$$\alpha_{xx,2D}^{\text{Slope}}(N_z + \Delta/2) = \frac{1}{\Delta}\big[\alpha_{xx,2D}^{\text{GME}}(N_z + \Delta) - \alpha_{xx,2D}^{\text{GME}}(N_z)\big]. \tag{43b}$$

The $\alpha_{xx,2D}^{\text{OBC}}$ is just the layer averaged GME coefficient. When $\Delta = 1$, we have $\alpha_{xx,2D}^{\text{Slope}} \approx \partial\alpha_{xx,2D}^{\text{GME}}/\partial N_z$, which stands for the increasing of GME coefficient for an additional layer
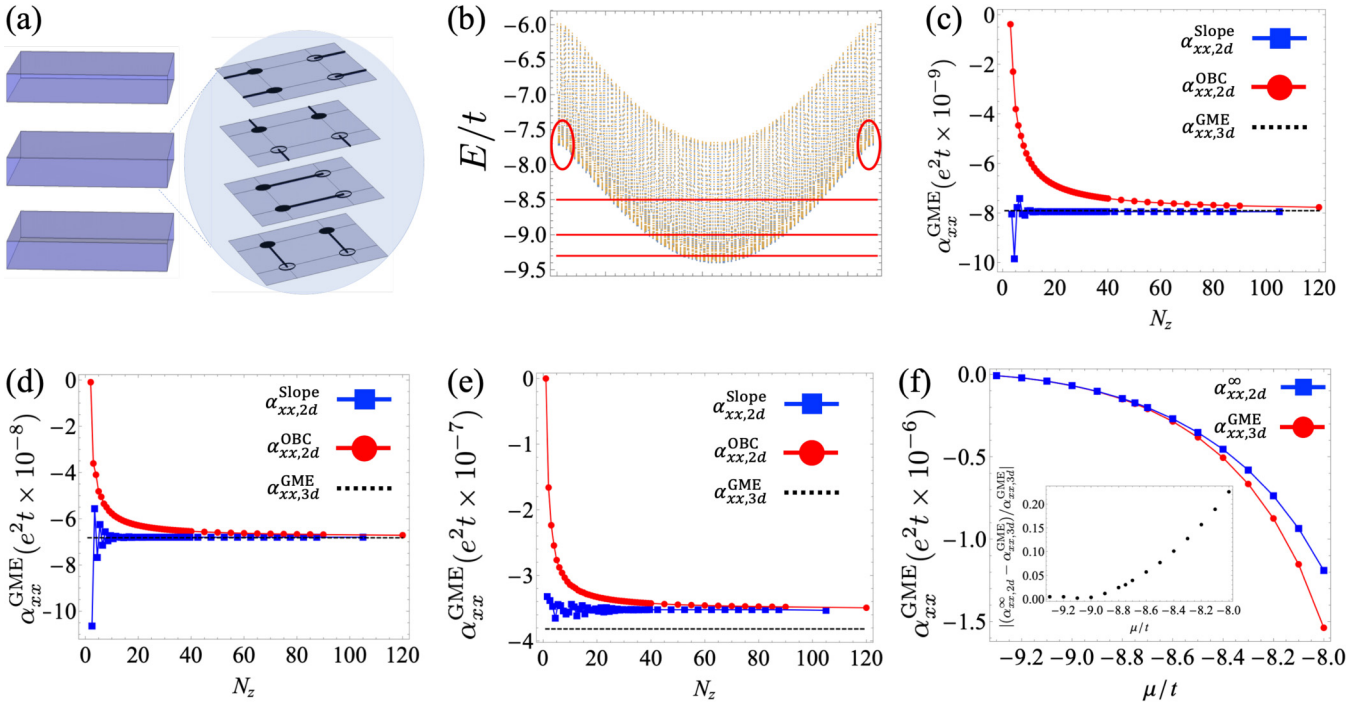
FIG. 3. Sketch for the 16-band model and numerical results. (a) Left: the sketch for layer stacking; right: the configuration for each unit cell. Note that each layer itself has some structure along $\hat{e}_z$ direction. (b) The 2D band structure of a 15 layers slab for the lowest 7 sub-bands. Note that the 2D band structure should be understood as following: we assign each **k** point (k_x, k_y) with a unique label, such that all **k** points form a one-dimensional array. The y axis stands for the energy, while the x axis stands for the label for **k** points. The red lines in the figure from the bottom to the top stand for Fermi level in (c)–(e), respectively. The red circles highlight the band touching points. (c)–(e) The GME coefficient for the 16 bands model Eq. [(45)], with $t = 1.0$, $t_z = 3.0t$, $\delta t = \epsilon = 0.4t$, and $k_B T = 0.03t$. The blue, red, and black line denotes, respectively, the slope/averaged value for α_{xx} based on Eq. [(43)], and 3D infinite volume results for Bloch electron based on Eq. [(39)]. The subfigures (c) $\mu = -9.3t$, the difference compared with 3D result is $|(\alpha_{xx,2D}^\infty - \alpha_{xx,3D}^{GME})/\alpha_{xx,3D}^{GME}| \approx 0.5\%$, (d) $\mu = -9.0t$, the difference compared with 3D result is $|(\alpha_{xx,2D}^\infty - \alpha_{xx,3D}^{GME})/\alpha_{xx,3D}^{GME}| \approx 0.4\%$, (e) $\mu = -8.5t$, and the difference compared with the 3D result is $|(\alpha_{xx,2D}^\infty - \alpha_{xx,3D}^{GME})/\alpha_{xx,3D}^{GME}| \approx 7.4\%$. (f) The $\alpha_{xx,2D}^\infty$ and $\alpha_{xx,3D}^{GME}$ with respect to different Fermi levels. The relevant difference between 2D and 3D results is increased as more bands become close in energy, as shown in the subfigure.

based on a N_z-layer slab. In large N_z limit, $\alpha_{xx,2D}^{OBC}$ and $\alpha_{xx,2D}^{Slope}$ will converge to the same value by their definition, and we denote that as $\alpha_{xx,2D}^\infty$, i.e.:

$$\alpha_{xx,2D}^\infty = \lim_{N_z \to \infty} \alpha_{xx,2D}^{OBC}(N_z) = \lim_{N_z \to \infty} \alpha_{xx,2D}^{Slope}(N_z). \quad (44)$$

In this section, we use a tight-binding model to verify that $\alpha_{xx,2D}^\infty$ converges to $\alpha_{xx,3D}^{GME}$ if the Fermi level is away from band touchings, which are inevitable in a time-reversal symmetric system.

Consider the following tight-binding Hamiltonian [2]:

$$\mathcal{H}_0 = -t \sum_{\langle ij \rangle} (c_i^\dagger c_j + c_j^\dagger c_i)$$
$$- \delta t \sum_{b \in B} (c_{b1}^\dagger c_{b2} + c_{b2}^\dagger c_{b1}) + \epsilon \sum_{s \in S} c_s^\dagger c_s. \quad (45)$$

Each unit cell contains 16 sites dispersed on four separated sheets along $\hat{e}_z$ direction, as shown in Fig. 3(a). The subscripts i and j label sites of a nearest-neighbor bond with the nearest-neighbor hopping t. The nonzero on-site potential ϵ and thick bonds are added to make the model chiral and break the inversion symmetry. The thick bonds are labeled by B, the sites at two ends of a bond $b \in B$ are labeled by $b1$ and $b2$,

and the set of solid-circle sites S. There is a screw axis parallel to $\hat{e}_z$ and passing through the upper-left sites in Fig 3(a). Here, the distance between one site and its nearest neighbor is denoted as a.

In the quasi-2D formula Eq. (31), the position operator used in open boundary calculation reads: $\hat{z} = \{a, a, a, a, 2a, 2a, 2a, 2a, \cdots, 4N_z a, 4N_z a, 4N_z a, 4N_z a\}$. One can make this kind of unit cell periodic extensively in the x-y plane, as in the blue layer shown in the left part of Fig. 3(a), and stack N_z identical layers, which share the same screw axis along the $\hat{e}_z$ direction. The interlayer coupling is just the nearest-neighbor hopping t. For the open (free) boundary condition, the uppermost layer and lowest layer are decoupled, from which we can get $\alpha_{xx,2D}^{OBC}(N_z)$ and $\alpha_{xx,2D}^{Slope}(N_z)$ from Eq. [(31)]. The results of $\alpha_{xx,2D}^{OBC}$, $\alpha_{xx,2D}^{Slope}$, and $\alpha_{xx,3D}^{GME}$ are presented in Figs. 3(c)–3(e) for different Fermi levels.

One thing that we would like to point out is that Eq. (29) [thus Eq. (31)] does not apply if there is any degeneracy for 2D bands at certain $\tilde{\mathbf{k}}$. On the other hand, at these $\tilde{\mathbf{k}}$ there must be a value for Eq. (28) from using velocity operator $\hat{v}_z$, which may be different from the result if we directly use Eq. (31). One can see that as the Fermi level is tuned to the band bottom of lowest sub-band (away from the band touching points), the

difference between the 2D results and 3D results is very small, in Figs. 3(c)–3(d), 3(f).

VI. CONCLUSION

In conclusion, based on standard perturbation theory, we derived a formula that evaluates the GME coefficient (i.e., optical rotation) for 2D thin chiral/twisted materials in the low-frequency limit. The formula is associated with the $\hat{z}$ position operator but extended states in the x and y directions, and can be easily applied in any 2D tight-binding model. We further provided a Feynman diagrammatic interpretation for our formula, which helps to give it a straightforward physical meaning. Finally, we showed the convergence of the 2D formula in the thermodynamic limit to 3D bulk results.

The prediction of optical rotation based on this formula will be useful in current and future experiments, such as for determining the chiralities of materials with different handed-ness and the size of the twist angle or, conversely, the rotation angle produced for a given twist. Two possible extensions are to combine the results with tight-binding parametrizations produced by modern electronic-structure calculations and to generalize the results to the case of band touchings at the Fermi level and to Moiré systems without a unit cell.

[1] L. Landau and E. M. Lifshitz, *Electrodynamics of Continuous Media* (Pergamon Press, New York, 1984) .

[2] J. Orenstein and J. E. Moore, Phys. Rev. B **87**, 165110 (2013).

[3] S. Zhong, J. E. Moore, and I. Souza, Phys. Rev. Lett. **116**, 077201 (2016).

[4] V. M. Agranovich and V. L. Ginzburg, *Crystal Optics with Spatial Dispersion, and Excitons*, 2nd ed. (Springer, Berlin, 1984).

[5] D. T. Son and N. Yamamoto, Phys. Rev. Lett. **109**, 181602 (2012).

[6] P. Goswami and S. Tewari, arXiv:1311.1506.

[7] M.-C. Chang and M.-F. Yang, Phys. Rev. B **91**, 115203 (2015).

[8] J. Ma and D. A. Pesin, Phys. Rev. B **92**, 235205 (2015).

[9] F. Flicker, F. de Juan, B. Bradlyn, T. Morimoto, M. G. Vergniory, and A. G. Grushin, Phys. Rev. B **98**, 155145 (2018).

[10] P. Goswami, G. Sharma, and S. Tewari, Phys. Rev. B **92**, 161110(R) (2015).

[11] S. S. Tsirkin, P. A. Puente, and I. Souza, Phys. Rev. B **97**, 035158 (2018).

[12] M. M. Vazifeh and M. Franz, Phys. Rev. Lett. **111**, 027201 (2013).

[13] N. Yamamoto, Phys. Rev. D **92**, 085011 (2015).

[14] Y. Chen, S. Wu, and A. A. Burkov, Phys. Rev. B **88**, 125105 (2013).

[15] L. Wu, S. Patankar, T. Morimoto, N. L. Nair, E. Thewalt, A. Little, J. G. Analytis, J. E. Moore, and J. Orenstein, Nat. Phys. **13**, 350 (2017).

[16] F. de Juan, A. G. Grushin, T. Morimoto, and J. E. Moore, Nature Commun. **8**, 15995 (2017).

[17] D. Rees, K. Manna, B. Lu, T. Morimoto, H. Borrmann, C. Felser, J. E. Moore, D. H. Torchinsky, and J. Orenstein, arXiv:1902.03230.

[18] A. Avdoshkin, V. Kozii, and J. E. Moore, arXiv:1912.02193 .

[19] R. W. Havener, H. Zhuang, L. Brown, R. G. Hennig, and J. Park, Nano Lett. **12**, 3162 (2012).

[20] C.-J. Kim, A. Sánchez-Castillo, Z. Ziegler, Y. Ogawa, C. Noguez, and J. Park, Nature Nanotechnol. **11**, 520 (2016).

[21] F. Crasto de Lima, G. J. Ferreira, and R. H. Miwa, Nano Lett. **19**, 6564 (2019).

[22] J. M. B. Lopes dos Santos, N. M. R. Peres, and A. H. Castro Neto, Phys. Rev. Lett. **99**, 256802 (2007).

[23] R. Bistritzer and A. H. MacDonald, Proc. Nat. Acad. Sci. **108**, 12233 (2011).

[24] J. M. B. Lopes dos Santos, N. M. R. Peres, and A. H. Castro Neto, Phys. Rev. B **86**, 155449 (2012).

[25] Y. Cao, V. Fatemi, S. Fang, K. Watanabe, T. Taniguchi, E. Kaxiras, and P. Jarillo-Herrero, Nature (London) **556**, 43 (2018).

[26] Y. Cao, V. Fatemi, A. Demir, S. Fang, S. L. Tomarken, J. Y. Luo, J. D. Sanchez-Yamagishi, K. Watanabe, T. Taniguchi, E. Kaxiras, R. C. Ashoori, and P. Jarillo-Herrero, Nature (London) **556**, 80 (2018).

[27] C. Xu and L. Balents, Phys. Rev. Lett. **121**, 087001 (2018).

[28] H. C. Po, L. Zou, A. Vishwanath, and T. Senthil, Phys. Rev. X **8**, 031089 (2018).

[29] N. F. Q. Yuan and L. Fu, Phys. Rev. B **98**, 045103 (2018).

[30] M. Koshino, N. F. Q. Yuan, T. Koretsune, M. Ochi, K. Kuroki, and L. Fu, Phys. Rev. X **8**, 031087 (2018).

[31] H. Isobe, N. F. Q. Yuan, and L. Fu, Phys. Rev. X **8**, 041041 (2018).

[32] Y. Gao, Y. Zhang, and D. Xiao, Phys. Rev. Lett. **124**, 077401 (2020).

[33] Z. Addison, J. Park, and E. J. Mele, Phys. Rev. B **100**, 125418 (2019).

[34] E. S. Morell, L. Chico, and L. Brey, 2D Materials **4**, 035015 (2017).

[35] T. Thonhauser, D. Ceresoli, D. Vanderbilt, and R. Resta, Phys. Rev. Lett. **95**, 137205 (2005).

[36] D. Ceresoli, T. Thonhauser, D. Vanderbilt, and R. Resta, Phys. Rev. B **74**, 024408 (2006).

[37] D. Xiao, J. Shi, and Q. Niu, Phys. Rev. Lett. **95**, 137204 (2005).

[38] J. Shi, G. Vignale, D. Xiao, and Q. Niu, Phys. Rev. Lett. **99**, 197202 (2007).

[39] T. Yoda, T. Yokoyama, and S. Murakami, Sci. Rep. **5**, 12024 (2015).

[40] W.-Y. He, D. Goldhaber-Gordon, and K. T. Law, Nat. Commun. **11**, 1650 (2020).

[41] A. L. Sharpe, E. J. Fox, A. W. Barnard, J. Finney, K. Watanabe, T. Taniguchi, M. A. Kastner, and D. Goldhaber-Gordon, Science **365**, 605 (2019).

[42] M. Serlin, C. L. Tschirhat, H. Polshyn, Y. Zhang, J. Zhu, K. Watanabe, T. Taniguchi, L. Balents, and A. F. Young, Science **367**, 900 (2020).

[43] R. Bianco and R. Resta, Phys. Rev. B **84**, 241106(R) (2011).

[44] R. Bianco and R. Resta, Phys. Rev. Lett. **110**, 087202 (2013).

[45] D. E. Parker, T. Morimoto, J. Orenstein, and J. E. Moore, Phys. Rev. B **99**, 045121 (2019).

[46] T. Holder, D. Kaplan, and B. Yan, arXiv:1911.05667.

[47] E. Blount, Solid State Phys. **13**, 305 (1962).

[48] R. M. Hornreich and S. Shtrikman, Phys. Rev. **171**, 1065 (1968).

[49] A. Malashevich and I. Souza, Phys. Rev. B **82**, 245118 (2010).

[50] F. Wooten, *Optical Properties of Solids* (Academic Press, New York, 1972) .

[51] M. Dressel and G. Grúner, *Electrodynamics of Solids* (Cambridge University Press, Cambridge, 2002) .

[52] W. A. Harrison, *Solid State Theory* (Dover, New York, 1980).

[53] D. B. Melrose and R. C. McPhedran, *Electromagnetic Processes in Dispersive Media* (Cambridge University Press, Cambridge, 1991) .

[54] P. B. Allen, S. G. Louie, and M. L. Cohen, Chapter 6 electron transport, *Contemporary Concepts of Condensed Matter Science* (Elsevier, 2006), Vol. 2, pp. 165–218.

[55] Y. Yafet, Phys. Rev. **106**, 679 (1957).

[56] B. Gu, N. H. Kwong, and R. Binder, Phys. Rev. B **87**, 125301 (2013).

[57] R. Resta, Phys. Rev. Lett. **80**, 1800 (1998).

[58] R. Yu, X. L. Qi, A. Bernevig, Z. Fang, and X. Dai, Phys. Rev. B **84**, 075119 (2011).